Serviceability Performance of Externally Prestressed Steel-Concrete Composite Girders

Assist. Prof. Dr. Nazar Kamil Ali Oukaili
Head of Civil Engineering Department
College of Engineering
University of Baghdad
E-mail:- dr_nazar12000@yahoo.com

Assist. Lect. Mustafa Kamil Buniya
E-mail:- mu_ka_1987@yahoo.com

ABSTRACT
The behavior of externally prestressed composite beams under short term loading has been studied. A computer program developed originally by Oukaili to evaluate curvature is modified to evaluate the deflection of prestressed composite beam under flexural load. The analysis model based on the deformation compatibility of entire structure that allows to determine the full history of strain and stress distribution along cross section depth, deflection and stress increment in the external tendons .. The evaluation of curvatures for the composite beam involves iterations for computing the strains vectors at each node at any loading stage. The stress increment determined using equations depended on the member deflection at points of connection. The stress increment determined using equations depended on the member deflection at points of connection. The proposed model results for load – deflection response are compared with experimental data taken from Auyyb's beams. For beams with straight tendon profile the average discrepancy reached 5.77%, 8.48% and 5.23% corresponding to the 0.25, 0.5 and 0.75 of the maximum load, respectively. For beams with the draped tendon profile, the average discrepancy of the analytical deflections values reached 15.5%, 5.8% and 6.45% corresponding to the 0.25, 0.5 and 0.75 of maximum load, respectively.

KEYWORDS: Serviceability Performance, Composite Girders, External Prestress, Deviator, Second order effect

الاداء الوظيفي للروافد المركبة من الحديد والخرسانة مسبقة الجهد خارجيا

الاستاذ المساعد الدكتور نزار كامل علي العقيلي
رئيس قسم الهندسة المدنية – جامعة بغداد

المدرس المساعد مصطفى كامل بنية

الخلاصة

تمت دراسة سلوك العتبات المركبة من الحديد والخرسانة مسبقة الجهد خارجيا تحت تأثير الاحمال القصيرة الامد. تم تطوير برنامج حسابي اقترحه العقيلي مسبقا لغرض حساب الهطول للعتبات المركبة تحت تأثير حمل الانحناء. .النموذج التحليلي المعتمد في هذا الدراسة يعتمد على مبدأ التوافق في التشوه للمنشأ الذي يمكننا من حساب الانفعالات والاجهادات على مدى ارتفاع المقطع العرضي , الهطول ,زيادة الاجهاد في الحديد مسبق الجهد خارجيا. إنّ اسلوب تحديد التقوس (curvature) للعتبة الإنشائية يتضمن عمليات تكرارية هدفها إيجاد قيمة الانفعالات المحورية في كل مرحلة تحميل .ان زيادة الاجهادات في الحديد مسبق الجهد خارجيا تم حسابها بالاعتماد على معادلات تعتمد على الهطول في نقاط الاتصال بين الحديد مسبق الجهد الخارجيا والعتبة. تمت مقارنة النتائج المستخرجة من النموذج التحليلي المقترح في هذه الدراسة مع البيانات المختبرية المتوفرة ،اظهرت المقارنة ان معدل الفرق بين القيم النظرية والمختبرية للهطول تحت تأثير حمل مقداره 25 % و 50% و75 % من حمل الفشل هو 5.77 % و 8.48% و 5.23 % على التوالي

للعتبات المسبقة الجهد بواسطة حديد وضع بشكل مستقيم ان معدل الفرق بين القيم النظرية والمختبرية للهطول تحت تأثير حمل مقداره 25 % و 50% و75 % من حمل الفشل هو15.5 % و5.8 % و6.45 % على التوالي للعتبات المسبقة الجهد بواسطة حديد وضع بشكل(Double draped) .

الكلمات الرئيسية : الاداء الوظيفي، الروافد المركبة، مسبق الاجهاد خارجيا، التأثير الثانوي .

INTRODUCTION

External pre-stressing may be defined as a prestress inducted by tendons located outside the beam section and not directly connected to the beam along its length, but only in some places, through deviators and end-anchorages. This type of pre-stressing can be applied to both new and existing structures, that have to be strengthened due to several reasons like: changes in use, deficiencies in design or construction and structural deterioration due to age (F.Osimani, 2004). The first use with external steel tendons was in the 1950s, but after that it lay dormant for some time. Now external prestressing techniques with steel tendons have been widely used with success to improve existing structures (H. Nordin, 2005). The deterioration of existing bridges due to increased traffic loading, progressive structural aging, and reinforcement corrosion from severe weathering conditions has become a major problem around the world. The number of heavy trucks and the traffic volume on these bridges have both risen to a level exceeding the values used at the time of their design, as a result of which many of these bridges are suffering fatigue damage and are therefore in urgent need of strengthening and repair. External prestressing is considered one of the most powerful techniques used for strengthening or rehabilitation of existing structures and had grown recently to occupy a significant share of the construction market. (Harajli et al, 1999).

A composite beam can be prestressed, using a jack, by tensioning high-strength tendons connected at both ends to brackets or anchorages that are fixed to the composite beam. Prestressing a composite beam can introduce internal stresses into the member cross sections that can be defined for different purposes. Such induced stresses can then counteract the external loads applied on the structure. Prestressing can be carried out for simple-span or continuous-span composite beams. The main advantages of prestressing steel members are the following:

- To enlarge the elastic range of behavior.
- To increase the ultimate capacity.
- To reduce the structural steel weight;

The first advantage results from the introduction of an internal moment couple acting in opposite direction to that induced by the externally applied loads. For example, prestressing a tensile member increases the yield load because, to reach yielding, the stress in the member has to change from initial compression to the yield stress in tension. Second, adding tendons to a steel member increases the ultimate capacity. However, prestressing the tendons has no effect on the ultimate capacity. The third advantage results from the substitution of high-strength steel tendons for lower strength structural steel. (H. Saadatmanesh et al, 1989) .

STRESS-STRAIN MODEL

The stress-strain relationship for concrete and steel takes the following form :

$$\sigma_m = \varepsilon_m E_m \nu_m \qquad (1)$$

Where σ_m : stress in material

ε_m : strain in material

E_m : modulus of elasticity of material

v_m : factor represents the ratio between the elastic strain to the total strain in material, in which ($E_m v_m$) represents the secant modulus of elasticity (Korpenko et al 1986)

MOMENT-CURVATURE MODEL ASSUMPTIONS

The proposed model for calculating the moment-curvature response depends on the following assumptions:

1. Strain in the concrete and reinforcement is proportional to the distance from the neutral axis (i. e., a plane section before bending remains plane after bending).
2. Concrete behavior in compression and in tension is assumed to follow Korpenko's model .
3. Steel behavior is considered to follow Korpenko's models .
4. All stresses in concrete and steel are related to secant modulus of elasticity.
5. Shear and torsion stresses are ignored
6. Perfect bond between steel girder and concrete deck slab (i.e. no slip between the slab and steel beam).
7. The Stresses in the interface area were neglected.
8. The effects of creep, shrinkage, and residual stresses in the steel beams were neglected .
9. Linear strain distribution is assumed across the section depth (Navier's law) .
10. The beam is considered as simply supported with symmetrical shape along the vertical centerline of the beam. This includes the type of loading and the beam cross section.

RELATIONS REQUIRED TO DETERMINE STRAINS VECTOR

A prestressed composite section is taken as a case study for determining the moment-curvature relation of structural composite members. The steel girders is distinguished by the subscript (g), prestressed steel (ps), non-prestressed steel (s). The space that is occupied by the section is assigned by the symbol A_T. In this space, there are areas occupied by steel girder, concrete , prestressed steel, and nonprestressed steel which are symbolized as A_g, A_c, A_{ps} and A_s respectively, as shown in figure (1)

$$A_T = A_g + A_c + A_{ps} + A_s \quad (2)$$

The external force, which is either normal force (prestressing force) or applied load (dead load + live load) , leads to change the general form of the element causing strain distribution at individual sections. The strain energy per unit length is determined by the following formula:

$$U^{(\ell)} = \frac{1}{2}\int_{A_T}(\sigma\varepsilon + \tau\gamma)A_T \quad (3)$$

$$\sigma = \bar{E}\,\varepsilon \quad (4)$$

$\bar{E}$ = secant modulus of elasticity of the material, which takes into account the initial stresses and strains, and it is calculated based on stress-strain diagrams for the materials.

$$\bar{E} = \begin{cases} \bar{E}_g, & x,y \in A_g \\ \bar{E}_c; & x,y \in A_c \\ \bar{E}_{ps}; & x,y \in A_{ps} \\ \bar{E}_s; & x,y \in A_s \end{cases} \quad (5)$$

Eq. (4) is substituted in Eq. (3). Shear stress and strain which appear in Eq. (3) are neglected. So Eq. (3) takes the following form:

$$U^{(\ell)} = \frac{1}{2}\int_{AT} \varepsilon\bar{E}\varepsilon\, dA_T \quad (6)$$

Because a linear strain distribution across the cross-section is assumed, so the third order vector will simulate the strain increment as in Eq. (7):

$$\mathcal{E} = \lambda Z^T \quad (7)$$

where:

$$\lambda = [\varepsilon_o \quad \psi_x \quad \psi_y]^T;\ Z = \begin{bmatrix} 1 \\ y \\ x \end{bmatrix}$$

Assuming that a plane cross section remains plane, the strain at any point can be expressed by the following relationship.

$$\varepsilon = \varepsilon_{mi} + \varepsilon_o + \psi_x y + \psi_y x \quad (8)$$

Considering Eq. (7), then Eq. (6) becomes as:

$$U^{(\ell)} = \frac{1}{2}\int_{A_T} \lambda^T Z \bar{E} Z^T \lambda \, dA_T \quad (9)$$

The matrix K is determined by the following:

$$K = \int_{A_T} Z \bar{E} Z^T dA_T \quad (10)$$

K= stiffness matrix relative to the selected reference coordinates.

To identify the loads related to the resultant axial strains, partial differentiation of the strain energy equation is taken as:

$$\left.\begin{aligned} \frac{\partial U^{(\ell)}}{\partial \varepsilon_o} = N = K_1\lambda;\ \frac{\partial U^{(\ell)}}{\partial \psi_x} = M_x = K_2\lambda; \\ \frac{\partial U^{(\ell)}}{\partial \psi_y} = M_y = K_3\lambda \end{aligned}\right\} \quad (11)$$

The general stiffness vectors K is determined by the following equation:

$$K_1 = \left\{\int_{A_T} \bar{E} dA_T,\ \int_{A_T} \bar{E} y dA_T,\ \int_{A_T} \bar{E} x dA_T\right\} \quad (12)$$

$$K_2 = \left\{\int_{A_T} \bar{E} y dA_T,\ \int_{A_T} \bar{E} y^2 dA_T,\ \int_{A_T} \bar{E} yx dA_T\right\} \quad (13)$$

$$K_3 = \left\{\int_{A_T} \bar{E} x dA_T,\ \int_{A_T} \bar{E} xy dA_T,\ \int_{A_T} \bar{E} x^2 dA_T\right\} \quad (14)$$

The direct integration of stiffness vectors elements K1, K2 , and K3 is unknown theoretically because the secant modulus of elasticity depends on the value of the resulted strains, and the strain gradient which is not equal to zero. Accordingly, numerical methods should be used. Therefore, the cross section is covered by mesh mostly with perpendicular lines. Average value of the stress (strain) is taken in each cell. So the infinite summation of the elements of section stiffness matrix is substituted by a finite summation, that its maximum value is equal to the number of developed mesh cells. Based on this, the matrix elements take the following form:

$$K_{11} = \sum_{i=1}^{k} \bar{E}_{gi} A_{gi} + \sum_{i=1}^{n} E_{ci} A_{ci} + \sum_{i=1}^{r} \bar{E}_{psi} A_{psi} + \sum_{i=1}^{j} \bar{E}_{si} A_{si} \quad (15)$$

$$K_{12} = K_{21} = \sum_{i=1}^{k} \bar{E}_{gi} A_{gi} y_{gi} + \sum_{i=1}^{n} E_{ei} A_{ei} y_{ci} + \sum_{i=1}^{r} \bar{E}_{psi} A_{psi} y_{psi} + \sum_{i=1}^{j} \bar{E}_{si} A_{si} y_{si} \quad (16)$$

$$K_{13} = K_{31} = \sum_{i=1}^{k} \bar{E}_{gi} A_{gi} x_{gi} + \sum_{i=1}^{n} E_{ei} A_{ei} x_{ci} + \sum_{i=1}^{r} \bar{E}_{psi} A_{psi} x_{psi} + \sum_{i=1}^{j} \bar{E}_{si} A_{si} x_{si} \quad (17)$$

$$K_{22} = \sum_{i=1}^{k} \bar{E}_{gi} A_{gi} y^2_{gi} + \sum_{i=1}^{n} E_{ci} A_{ci} y^2_{ci} + \sum_{i=1}^{r} \bar{E}_{psi} A_{psi} y^2_{psi} + \sum_{i=1}^{j} \bar{E}_{si} A_{si} y^2_{si} \quad (18)$$

$$K_{23} = \sum_{i=1}^{k} \bar{E}_{gi} A_{gi} x_{gi} y_{gi} + \sum_{i=1}^{n} \bar{E}_{ci} A_{ci} x_{ci} y_{ci} + \sum_{i=1}^{r} \bar{E}_{psi} A_{psi} x_{psi} y_{psi} + \sum_{i=1}^{j} \bar{E}_{si} A_{si} x_{si} y_{si} \quad (19)$$

$$K_{33} = \sum_{i=1}^{k} \bar{E}_{gi} A_{gi} x^2_{gi} + \sum_{i=1}^{n} \bar{E}_{ci} A_{ci} x^2_{ci} + \sum_{i=1}^{r} \bar{E}_{psi} A_{psi} x^2_{psi} + \sum_{i=1}^{j} \bar{E}_{si} A_{si} x^2_{si} \quad (20)$$

$\bar{E}$ = secant modulus of Elasticity:

$$\bar{E} = E\nu \quad (21)$$

Where :E = the initial modulus of elasticity for the material (steel girder, concrete , or steel) .

ν= Elastic strain factor and it expresses the ratios between the elastic strains to total strains.

The system (11) can be rewritten in another form to become:

$$[F] = [K(\lambda)] * [\lambda] \quad (22)$$

where [F]= load vector, include the prestressing load vector calculated next chapter and applied load vector with self-weight ;$[K(\lambda)]$= Stiffness matrix of the section ; $[\lambda]$=Strain vector.

EVALUATION OF STRAIN VECTOR AT DIFFERENT LOADING CYCLES

The direct iteration method is adopted to solve a non-linear problem in Eq. (22) for determination of the strain vector for a cross-section subjected to known forces and takes the following form as shown in figure. (2). In a simple linear elastic problems the strain vector can be obtain directly, While this solution cannot be achieved when non linearity is present in the stiffness matrix [K], which depend on the axial strain level Eq..(22). The strain vector can take the following expression :

$$[\lambda] = [K(\lambda)]^{-1}[F] \quad (23)$$

The external load was applied step-by-step. First iteration assuming that the material is linear, initially assuming the value of ($\lambda = 0$) to compute the stiffness matrix, then the axial strain is obtained as:

$$\left.\begin{aligned} &[\lambda_i] = [K(\lambda_{i-1})]^{-1}[F] \\ &\lambda_o = 0 \\ &i = 1,2,3, \ldots\ldots\ldots, \ldots\ldots\ldots \end{aligned}\right\} \quad (24)$$

the stiffness matrix is changed in each iteration accordingly to the strain vector. the iteration will be terminated when the difference between the λ_i and $\lambda_{i-1}$was satisfied according to the following equation :

$$\|\lambda_i - \lambda_{i-1}\| < \delta \quad (25)$$

Where : λ_i, λ_{i-1} = axial strain vector at current and previous iteration cycles at same load level ,respectively .δ= very small value . Programming flow chart is shown in figure (5).

EVALUATION OF DEFLECTIONS

The value of deflection is determined using the Newmark's numerical integration. In the case of a symmetrical simply supported beam, Eq. (26) can be used by considering the following symbols: ψ refers to the curvature M/EI, $\bar{\psi}$ refers to the equivalent concentrated load (or curvature in the real beam), $\theta_{(i)}$ refers to the shear (or average slope in the real beam between the points) i and $i+1$, Δ_i refers to deflection, subscript i refers to section number, c refers to section number in the center of the beam, and (dx) refers to segment length which is equal to the distance between two concentrated loads. For simply supported beam, there are no values of $\bar{\psi}$ in both ends; therefore these values can be substituted by zero.

$$\Delta_{(i)} = \sum_{n=1}^{i} (\theta_{(i)}) * dx \quad (26)$$

Where $i = 1,2,3 \ldots\ldots c-1$

$$\theta_{(j)} = \sum_{K=i+1}^{c-1} \bar{\psi}_k + \frac{\bar{\psi}_c}{2} \quad (27)$$

$\theta_{(j)}$ is dimensionless

$$\bar{\psi}_k = \frac{\Delta x}{12}(\psi_{(k-1)} + 10\psi_k + \psi_{(k+1)}) \quad (28)$$

Calculation of the Tendons Eccentricity.

The eccentricity variation of externally prestresses tendons (i.e., second order effect) mainly depends on the member deflection at points of connection (anchorages and deviators) and the profile of tendons and existence of deviators (Zhi-Qi and Liu, 2010). For simply support composite beams with external tendons the eccentricity can be expressed by

$$e_x = e_o - \Delta_x \quad (29)$$

Where : e_x = effective eccentricity. e_o= Initial eccentricity at the time of prestressing. Δ_x= change of eccentricity due to external load .

- **STRAIGHT TENDONS PROFILE**

The effective tendons eccentricity can be calculated as in Eq.(30) . as shown in figure (3)

$$e_x = e_s - \delta_x \quad (30)$$

Where : δ_x= deflection at section x . e_s= tendons eccentricity at support .

The prestressing force vector can be determined as in Eq.(31) :

$$\begin{bmatrix} N_p \\ M_{p,x} \\ M_{p,y} \end{bmatrix} = \begin{bmatrix} -F_p \\ -F_p * e_x \\ 0 \end{bmatrix} \quad (31)$$

- **DRAPED TENDONS AT MID SPAN**

In this case the beam had one deviator installed at mid span as shown in figure (4) , the effective tendons eccentricity can be calculated as in Eq.(32).

$$e_x = \frac{e_s(L/2-x)+e_m x}{L/2} - \delta_x + \frac{\delta_{mid}\, x}{L/2} \quad (32)$$

Where: e_s= eccentricity at support. e_m= eccentricity at mid span . δ_{mid}= deflection at mid span .

The prestressing force vector can be determined in Eq. (33):

$$\begin{bmatrix} N_p \\ M_{p,x} \\ M_{p,y} \end{bmatrix} = \begin{bmatrix} -F_p * \cos\alpha \\ -F_p * \cos\alpha * e_x \\ 0 \end{bmatrix} \quad (33)$$

Where : α = angle of tendon with the longitudinal axis of beam and calculated as

$$a = (e_d - e_s) + \delta_{mid} - e_s(1 - cos\theta_s)$$

$$b = \frac{L}{2} + (e_s) * sin\theta_s \; ; \; \alpha = tan^{-1}\left(\frac{a}{b}\right)$$

Where : θ_s= Rotation of beam at support .

- **DOUBLE DRAPED TENDONS**

This case is combined of two cases previously as show in figure (5), the expression which will be used to determine e_x can using Eq. (34) :

$$e_x = \begin{cases} \frac{e_s(x_{div}-x)+e_d x}{x_{div}} - \delta_x + \frac{\delta_d x}{x_{div}} & ; \; x \le x_{div} \\ e_d - \delta_x + \delta_d & ; \; x > x_{div} \end{cases} \quad (34)$$

The prestressing force vector can be determined :

$$\left.\begin{bmatrix} N_p \\ M_{p,x} \\ M_{p,y} \end{bmatrix} = \begin{bmatrix} -F_p * \cos\alpha \\ -F_p * \cos\alpha * e_x \\ 0 \end{bmatrix}; \; x \le x_{div}\right\} \quad (35)$$

$$\left.\begin{bmatrix} N_p \\ M_{p,x} \\ M_{p,y} \end{bmatrix} = \begin{bmatrix} -F_p \\ -F_p * e_x \\ 0 \end{bmatrix} \; ; \; x \le x_{div}\right\}$$

Calculation of Tendon's Stress

The following procedure lead to determine the stress increment in the prestressing tendon Δf_{ps}:

$$\Delta\varepsilon_{ps} = \frac{\Delta L}{L_o} = \frac{L_d - L_o}{L_o} \quad (36)$$

$$\varepsilon_{ps} = \varepsilon_{psi} + \Delta\varepsilon_{ps}$$

(37)

$$f_{ps} = E_{ps} * v_{ps} * \varepsilon_{ps}$$

(38)

$$\Delta f_{ps} = f_{ps} - f_{psi} \quad (39)$$

Where :

v_{ps}= Elastic strain factor and it expresses the ratios between the elastic strains to total strains as defined by Korpinko (1986).

L_o =is the tendon length between fixed points (anchorages or deviators with no slip of the tendons) before loading.

ΔL = is the increment of length of the tendon, due to the deflection of the beam.

COMPARISONS BETWEEN PROPOSED MODEL AND EXPERIMENTAL TESTS

Comparisons with the experimental tests of two steel–concrete composite beams prestressed by external tendons with two different profiles types. (Ayyub et al 1990). Figure (6) shows the profile and cross section of beam B Table (1) shows the mechanical properties of beams B and C. Reasonable agreement of the proposed model with the experimental data was found. In the elastic loading range, the neutral axis of the composite section was located within the steel beam that resulting compression stresses in concrete deck slab. After the steel beam yielded, the neutral axis migrated upward. Figure (7) shows the load deflection response of proposed model and experimental values. Figure (8) show strain at bottom fiber of steel beam . The failure occurred when the strain at the top flange of concrete reached ($\varepsilon_c = 0.00257$). Figure (9) shows the strain of the top fiber of concrete. the maximum value of the stress increment in prestressed strand reached($\Delta f_{ps} = 542.43$ MPa). The total stress in strand ($f_{ps} = 1578.27$ MPa), that means the strand still in the elastic range. Figure (10) shows the increment of stresses in strand. The analytical results show very good agreement with the experimental data.

Ayyub (1990), also tested beam C which has a double draped tendon. This beam is similar to the previous beam B but the tendon draped at two points under load point . The tendon was installed at the center of gravity of the beam (i.e. $e_s = 0$) at support and (e_d =30 mm) above bottom flange of steel beam at the pure moment region. The prestressing force is (267 kN). The initial prestress in the strand is ($f_{psi} = 957$ MPa; $f_{psi} = 0.51\, f_{pu}$). Figure (11) shows the load deflection response of proposed model and experimental values. Figure (12) show strain at bottom fiber of steel beam . The failure occurred when the strain at the top flange of concrete reached ($\varepsilon_c = 0.0033$). Figure (13) shows the strain of the top fiber of concrete. The maximum value of stress increment in prestressed strand is reached to ($\Delta f_{ps} = 616$ MPa). The total stress in the strand is $\Delta f_{ps} = 1573$ MPa. That means the strand still in the elastic range. Figure (14) shows the increment of stresses in strand.

Figure (15) shows the load versus deflection at mid span of prestressed and non prestressed composite beams, the behavior of two beam are linearly in the load-deflection curves before yielding the bottom flange of steel beam. The results show that the external prestressed tendon significantly increases the yield and ultimate load. Figure (16) shows the effect of compressive strength concrete slab on the load-deflection behavior of the selected beam. The results show that the beams with stronger concrete were more ductile (higher mid span deflection values were reached) than the ones with weaker concrete.

CONCLUSION

1. The proposed model which presented in this study shows to be capable of predicting the full history of deflection, strain in concrete and the stress increment in the external tendons and all internal steel for the prestressed composite beam under short-term loading .
2. The analytical results show very good agreement with the experimental data. For the beams has a straight tendon profile. The average discrepancy of the proposed model deflections reached 5.77%, 8.48% and 5.23% corresponding to the 0.25, 0.5 and 0.75 of the maximum load respectively. For the beams has a double draped tendon profile the average discrepancy of the analytical deflections values reached 15.5%, 5.8% and 6.45% corresponding to the 0.25, 0.5 and 0.75 of maximum load respectively.
3. Higher tendon eccentricity results in higher ultimate strength for the beams. Thus, if possible, tendons should be located below the bottom (tension) flange.

4. At the same tendon eccentricity there seem to be no significant differences between the behavior of the beams prestressed with draped tendons and the ones prestressed with straight tendons with no intermediate saddle points.
5. External prestressing increases the yield load and the ultimate load of composite beams about 19.23%
6. The beams which has high strength concrete show higher mid span deflection values than the beams has low strength concrete with higher ultimate load.

REFERENCES

- ***Al-HawWassi, IQbal F*** (2008) " Short Term Deflection of Ordinary , Partially Prestressed and GFRP Bars Reinforced concrete Beams" master thesis, civil Eng. Dep. college of engineering, university of Baghdad.
- ***Ayyub B.M, Sohn YG, Saadatmanesh H. Prestressed*** (1990) "Prestressed composite girders under positive moment." Journal of Structural Engineering, Vol. 116, No. 11.
- ***Filippo Osimani*** **,(** 2004) **"** The Use of Unbonded Tendons for Prestressed Concrete Bridges**"** Master Thesis at Department of Structural Engineering, Structural Design and Bridges Group, at the Royal Institute of Technology (KTH) in Stockholm.
- ***Håkan Nordin (2005***), "Strengthening structures with externally prestressed tendons " Literature review, Luleå University of Technology, Technical Report at Department of Civil and Environmental Engineering Division of Structural Engineering
- ***Harajli M., Khairallah N. and Nassif H***. (1999) "Externally Prestressed Members: Evaluation of Second-order Effects" Journal of Strutural Engineering, October 1999, pp 1151-1161.
- ***Korpenko, N. I., Mukhamediev, T.A. and Petrov, A. N.,*** (1986), "The Initial and Transformed Stress - Strain Diagrams of Steel and Concrete. " Special Publication, Stress-Strain Condition for Reinforced Concrete Construction, Reinforced Concrete Research Center, Moscow, 7 – 25, as cited in (Oukaili, 1997).
- ***Oukaili, Nazar K. Ali***, (1997), "Moment Capacity and Strength of Reinforced Concrete Members Using Stress-Strain Diagrams of Concrete and Steel", Journal of King Saud University, Vol. 10, pp. 23-44, (in Arabic).
- ***Saadatmanesh, H., Albrecht, P., and Ayyub, B. M****(1989b)* "Experimental study of prestressed composite beams." Journal of Structural Engineering, Vol.115, No 9.
- ***Saadatmanesh, H., Albrecht. P., and Ayyub, B. M***. (1989 a) "Analytical study of prestressed composite beams." Journal of Structural Engineering, Vol.115, No 9.

NOTATIONS

A_g	Area Steel girders
A_{ps}	Area of prestressing steel
B_x	First moment of cross-sectional area about x-axis
B_y	First moment of cross-sectional area about y-axis
M_x	Bed nding moment in OXZ level
M_y	Bending moment in OYZ level
N_p	Normal force due to prestress force
$M_{p,x}$	Moment in OXZ level due to prestress force
$M_{p,y}$	Moment in OYZ level due to prestress force
N	Normal force
ε	Strain
ψ_x	curvature of the member longitudinal axis in OYZ plane.
ψ_y	curvature of the member longitudinal axis in OXZ plane.
γ	Shear strain
δ_{mid}	Deflection of mid span

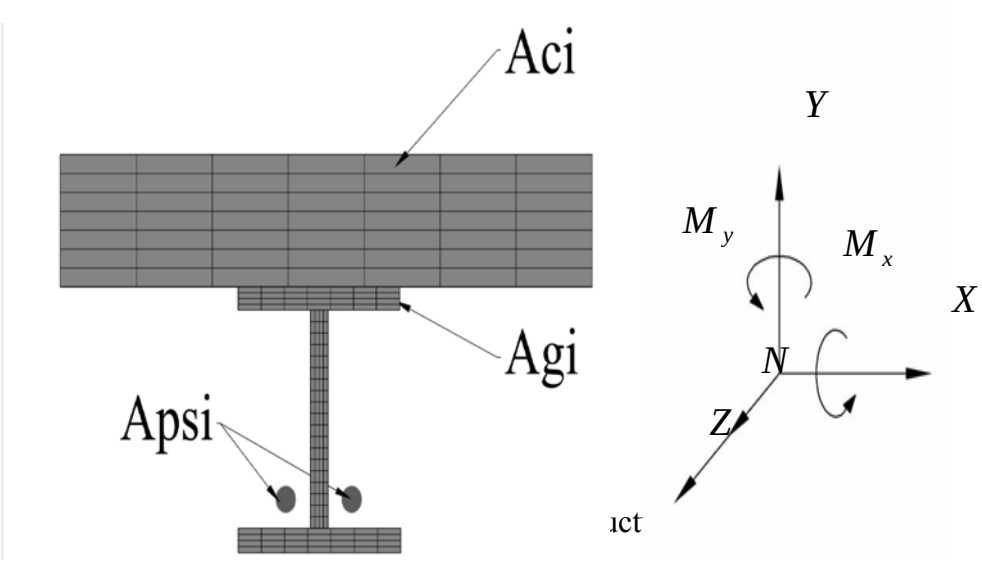

Figure (1): Cross-section of the structural element

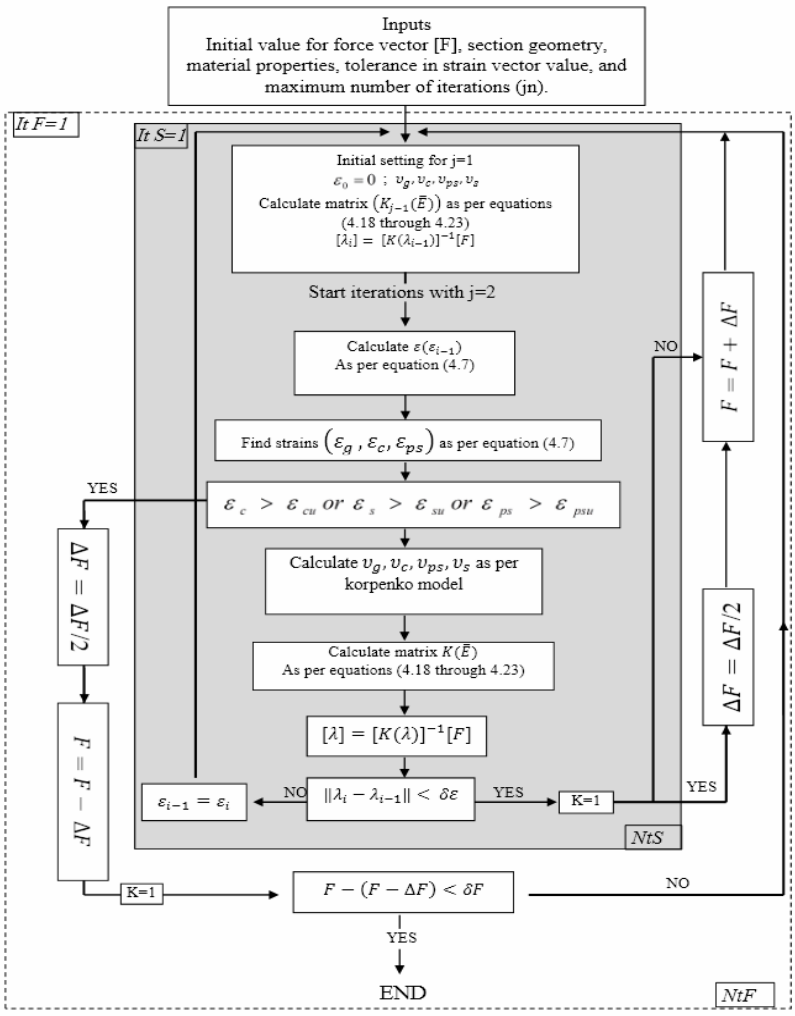

Figure (2): Flow chart for step by step procedure for determination of strain vector for a given load and determination of ultimate load

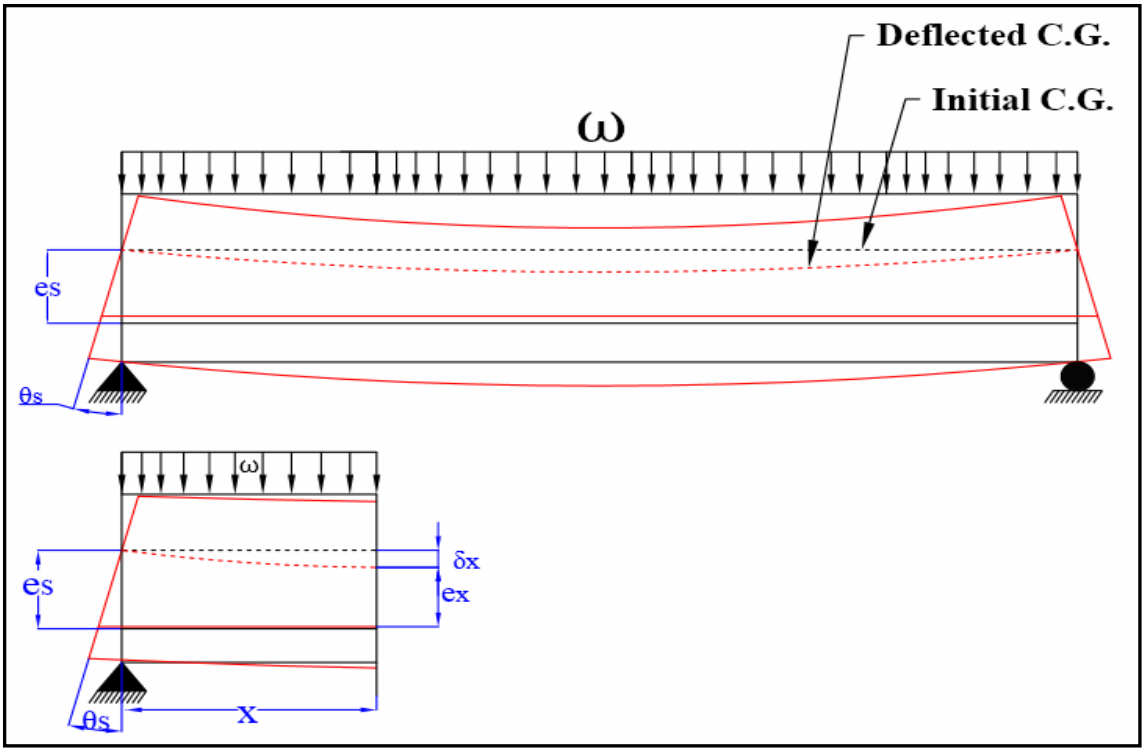

Figure (3): Straight tendon beam, a) loaded beam, b)eccentricity at distance X

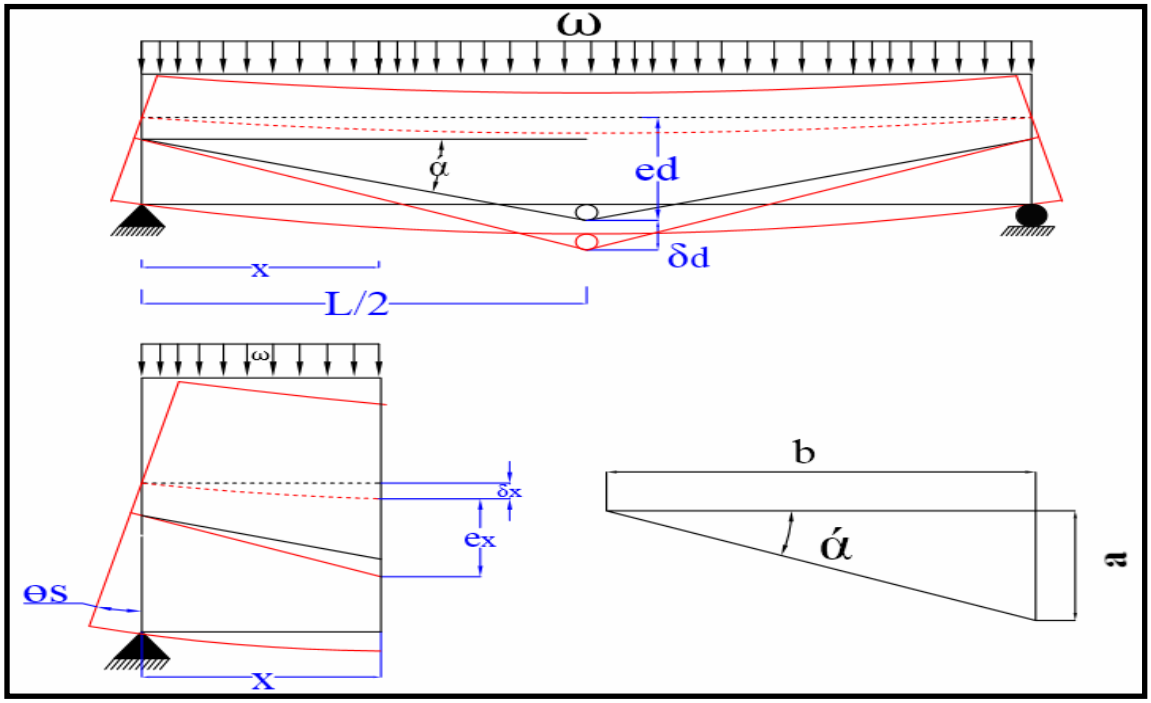

Figure (4): a)draped tendon beam, b)eccentricity at distance X, c) angle of tendon

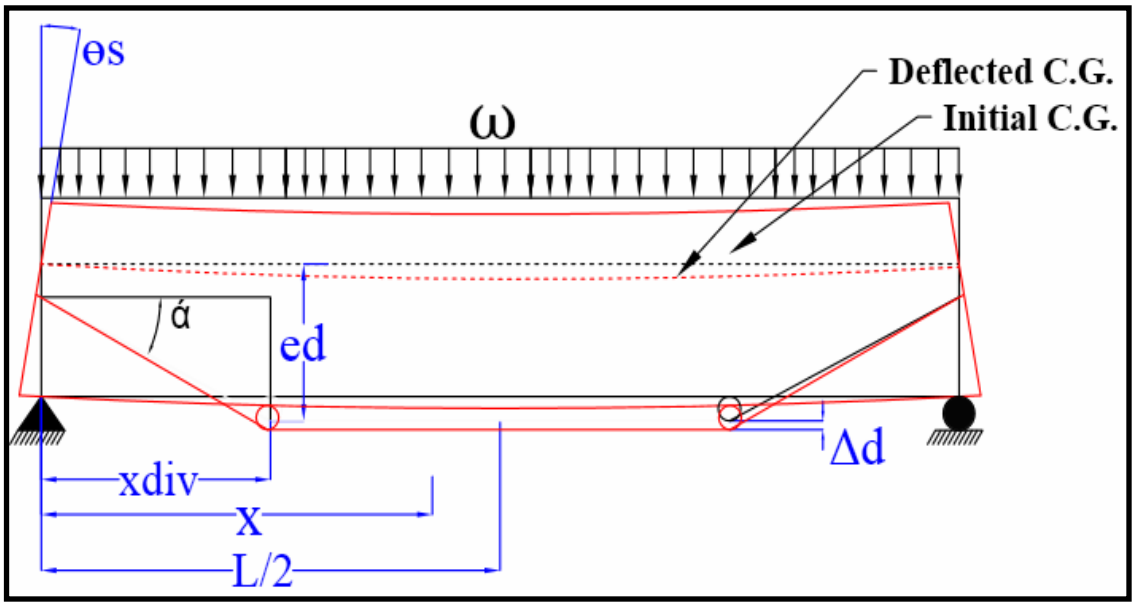

Figure (5): Double draped tendon

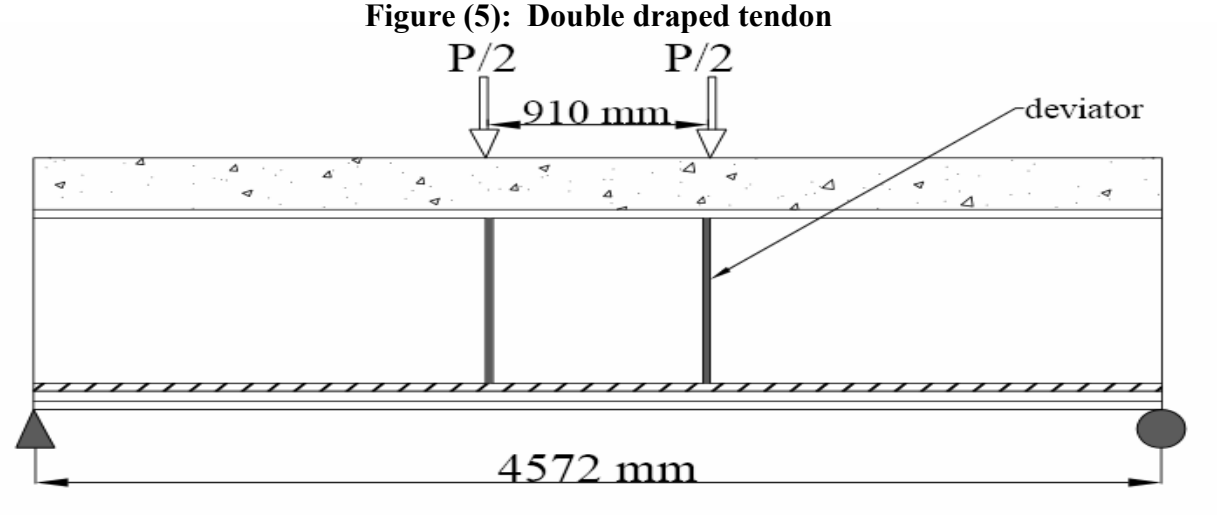

(a)

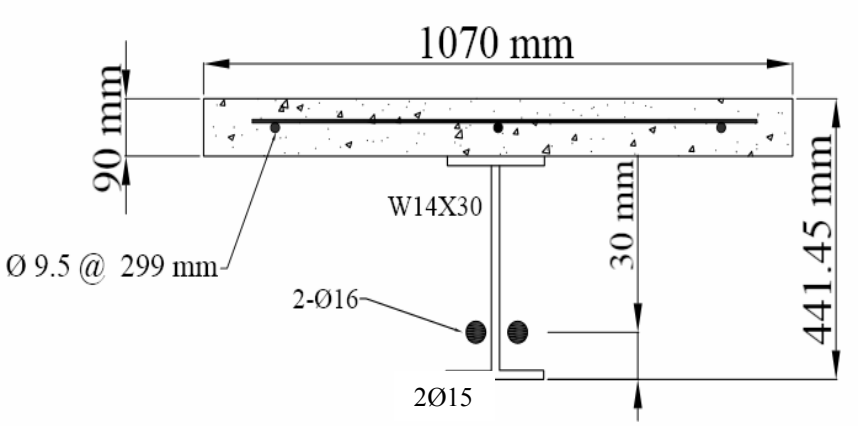

(b)

Figure (6): a) profile of beam B ,b)details of Beam B and C

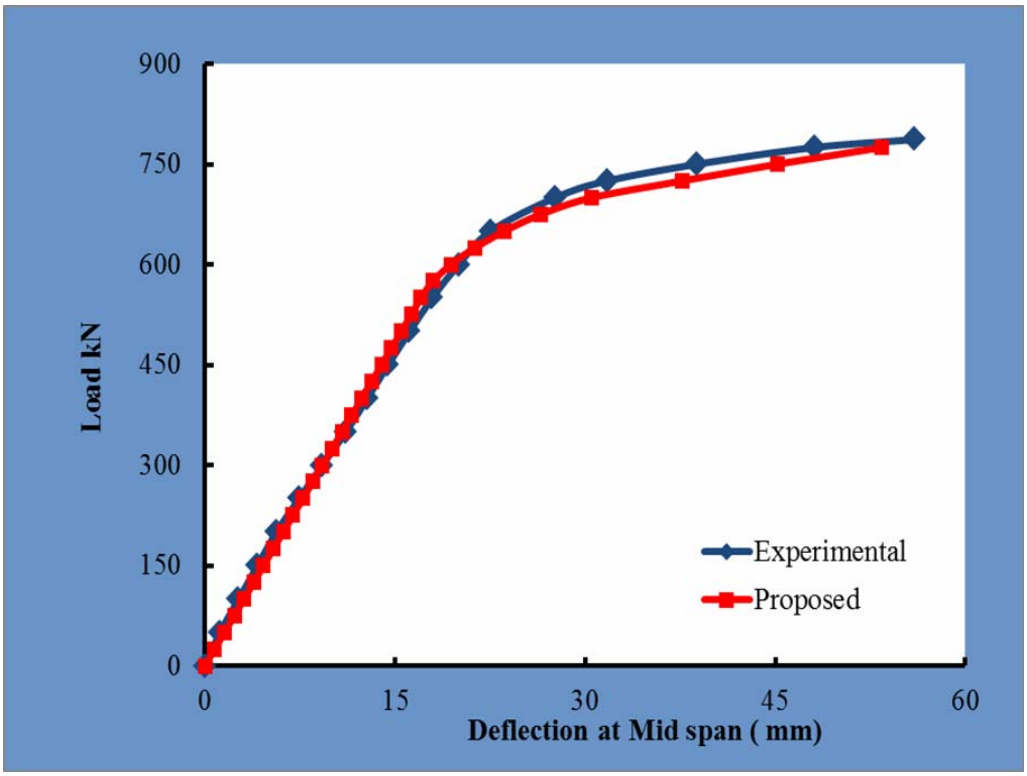

Figure (7): ;load-deflection response at midspan of beam B

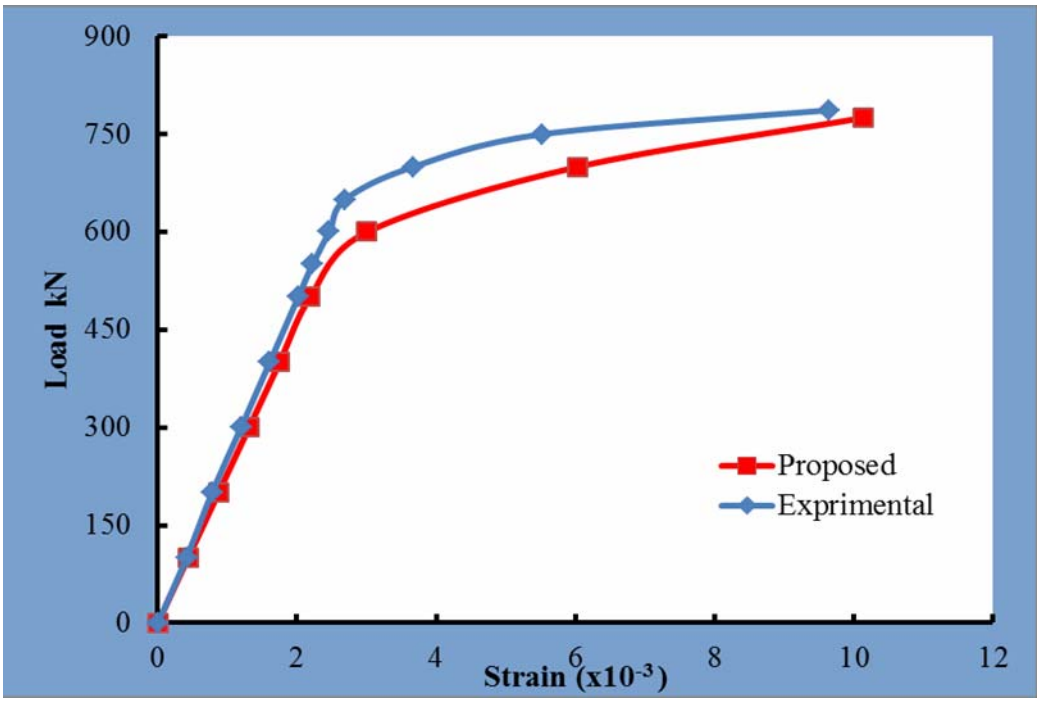

Figure (8): Load-Strain Curve for the bottom flange of steel beam at mid-span of beam B

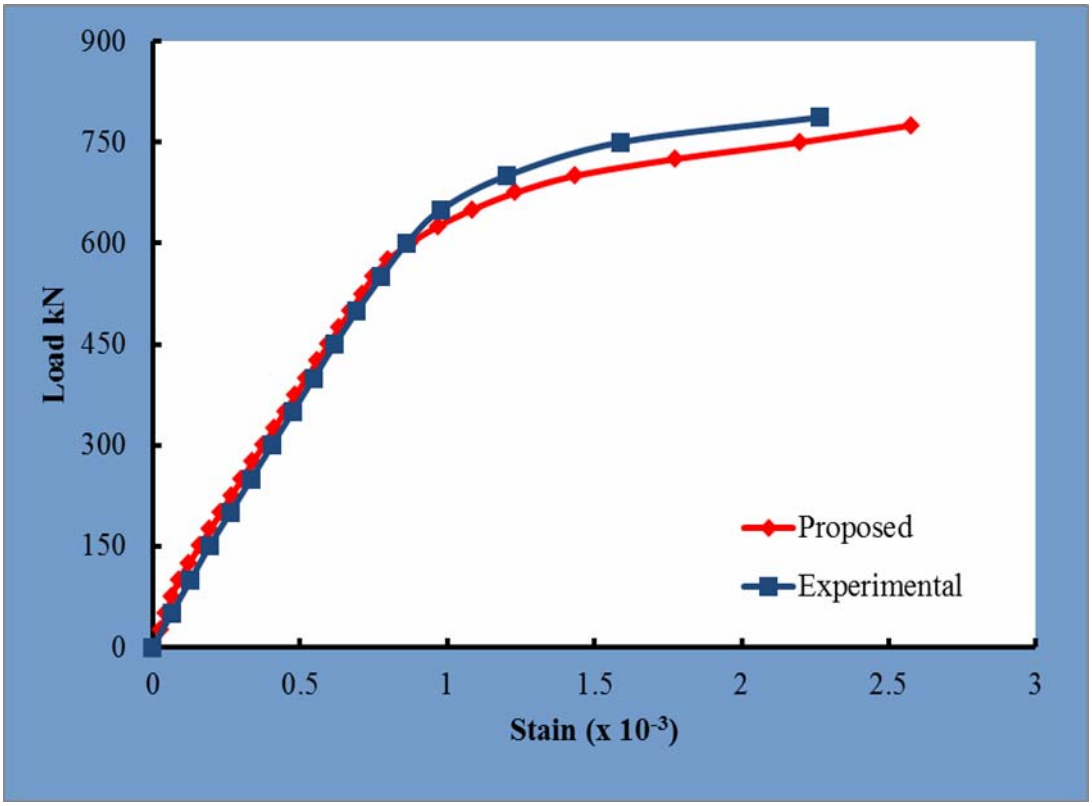

Figure (9): Load-Strain Curve for the top flang of Concrete, beam B.

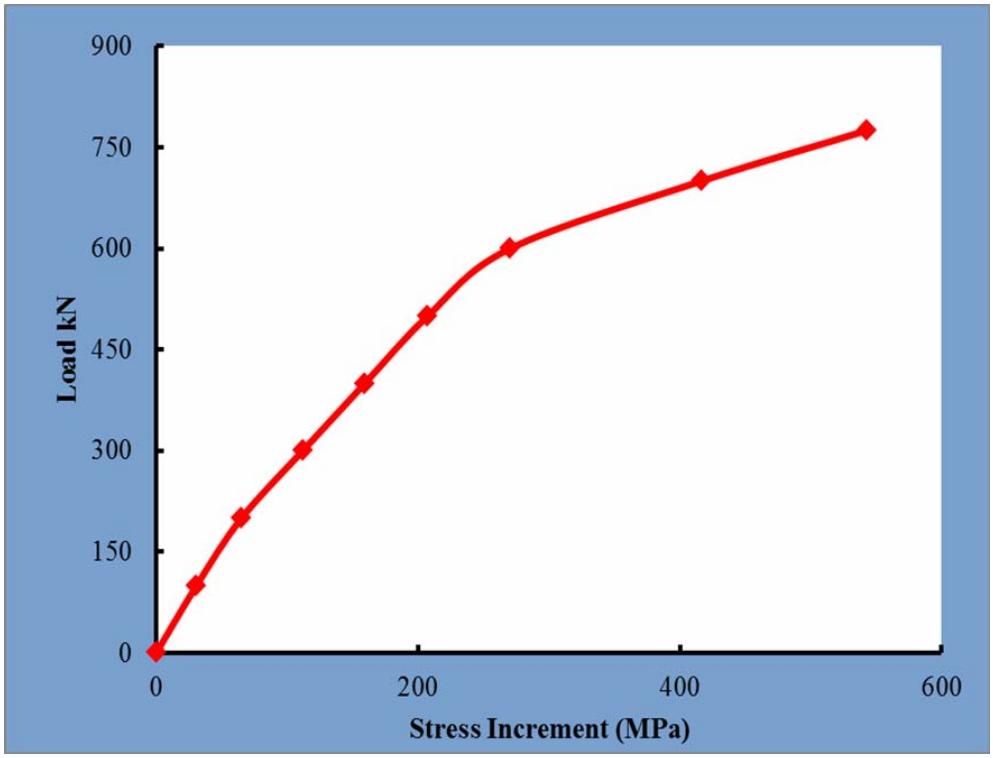

Figure (10): Stress increment in the Strand determined by the proposed model at beam B

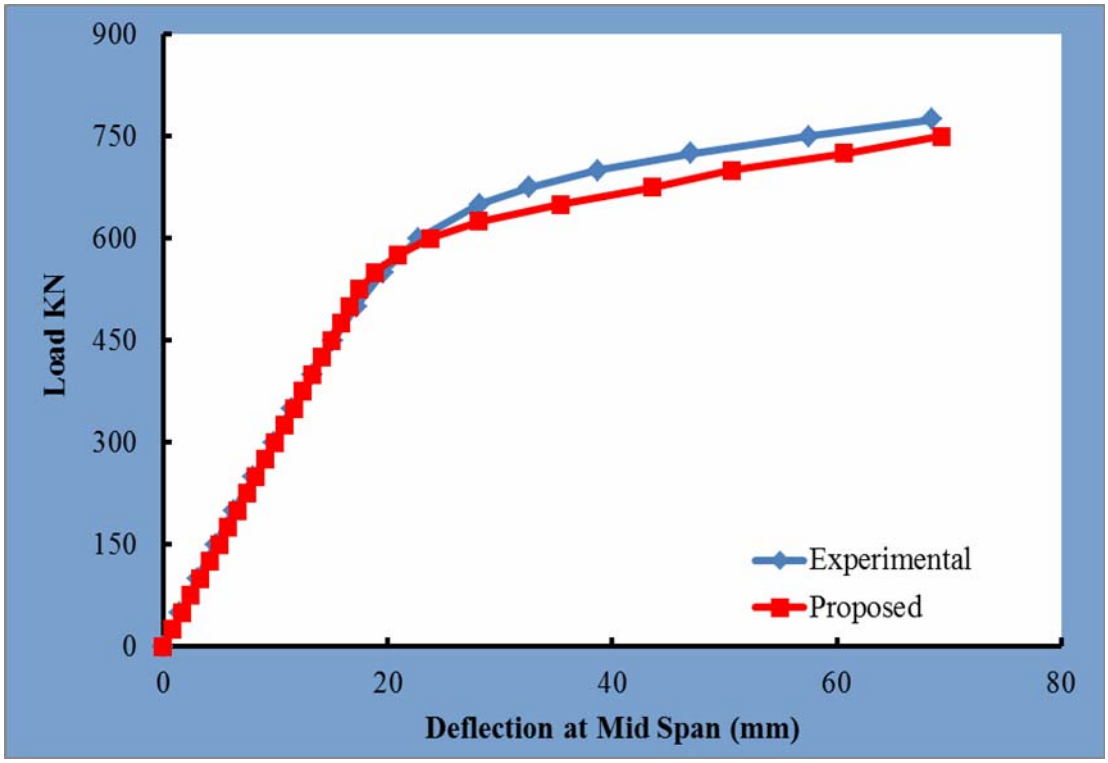

Figure (11): load deflection response for beam C

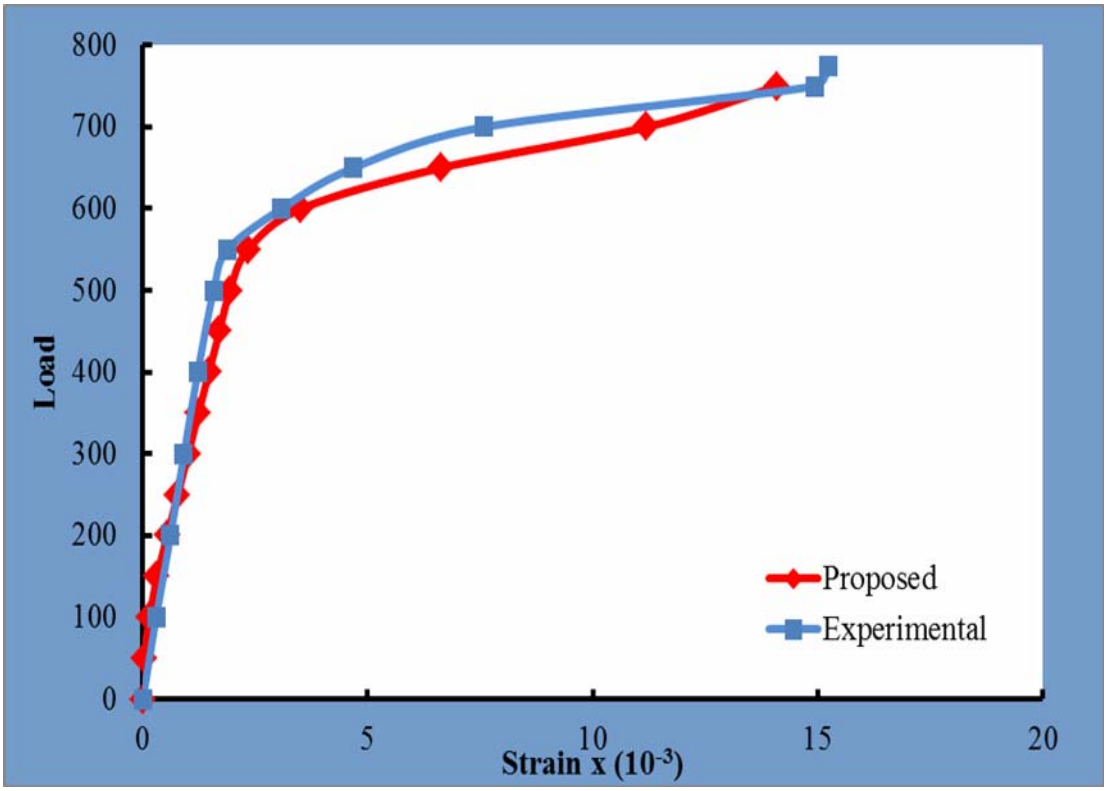

Figure (12): Load-Strain Curve for the bottom flange of steel beam at mid-span of beam B

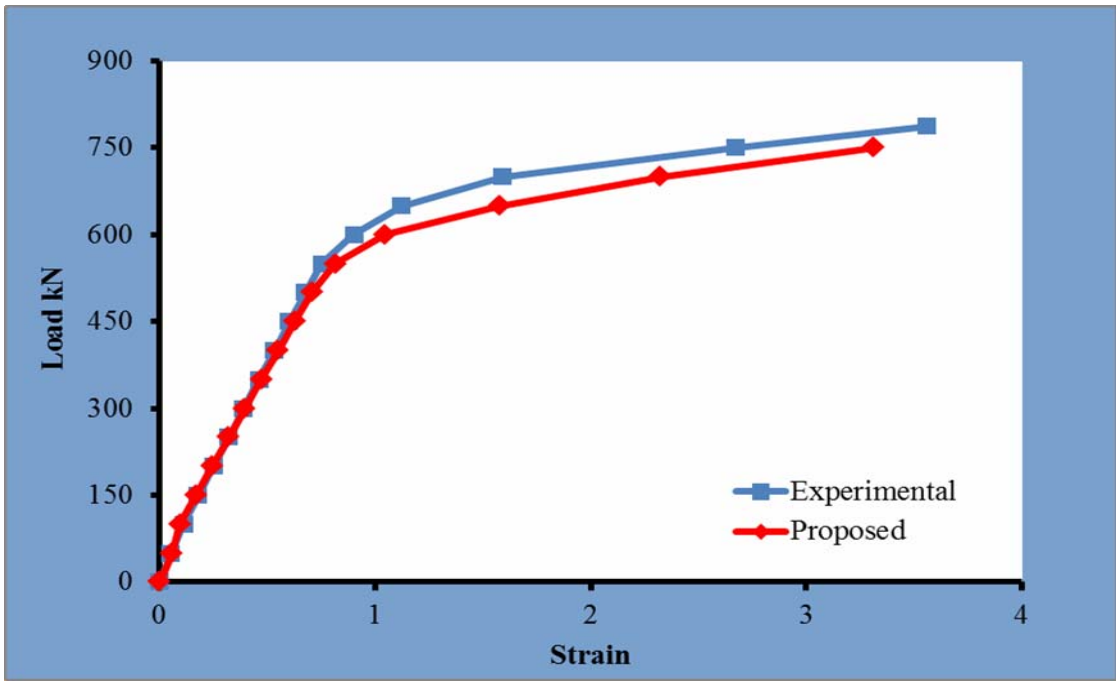

Figure (13): Load-strain curve of top flange in concrete deck slab of beam C

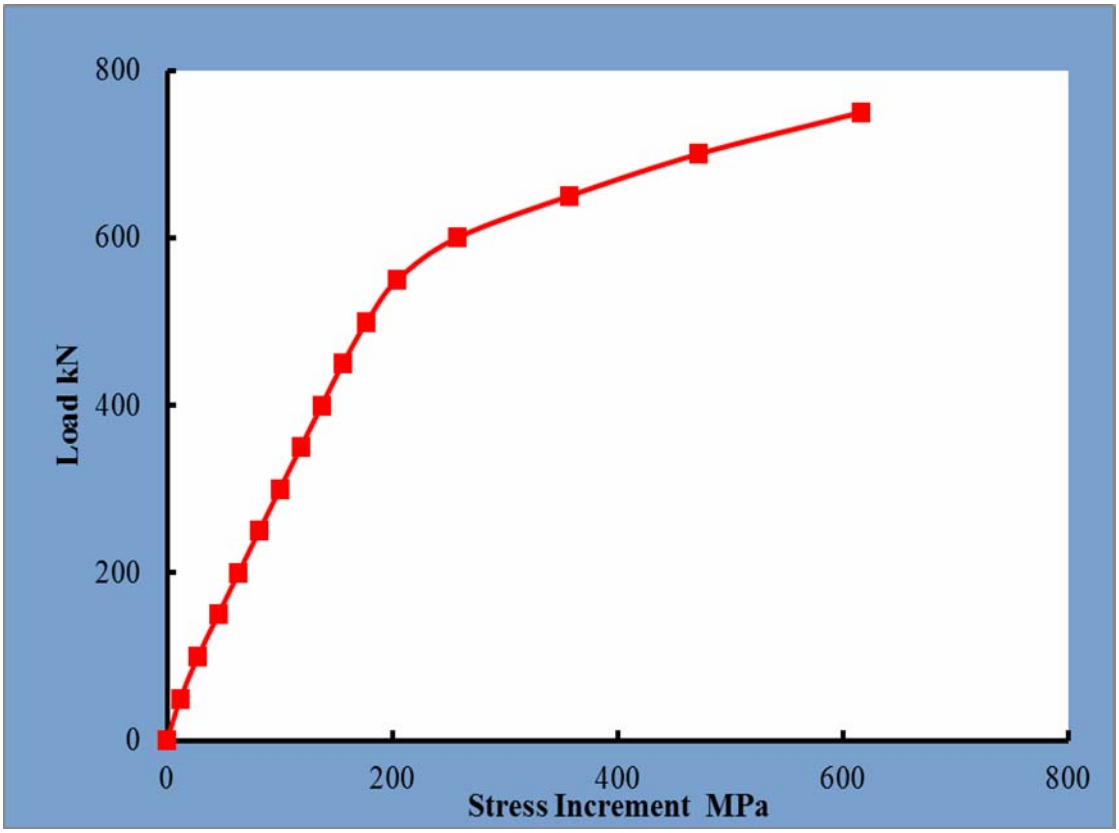

Figure (14): Stress increment in the Strand at beam C, determined by proposed model.

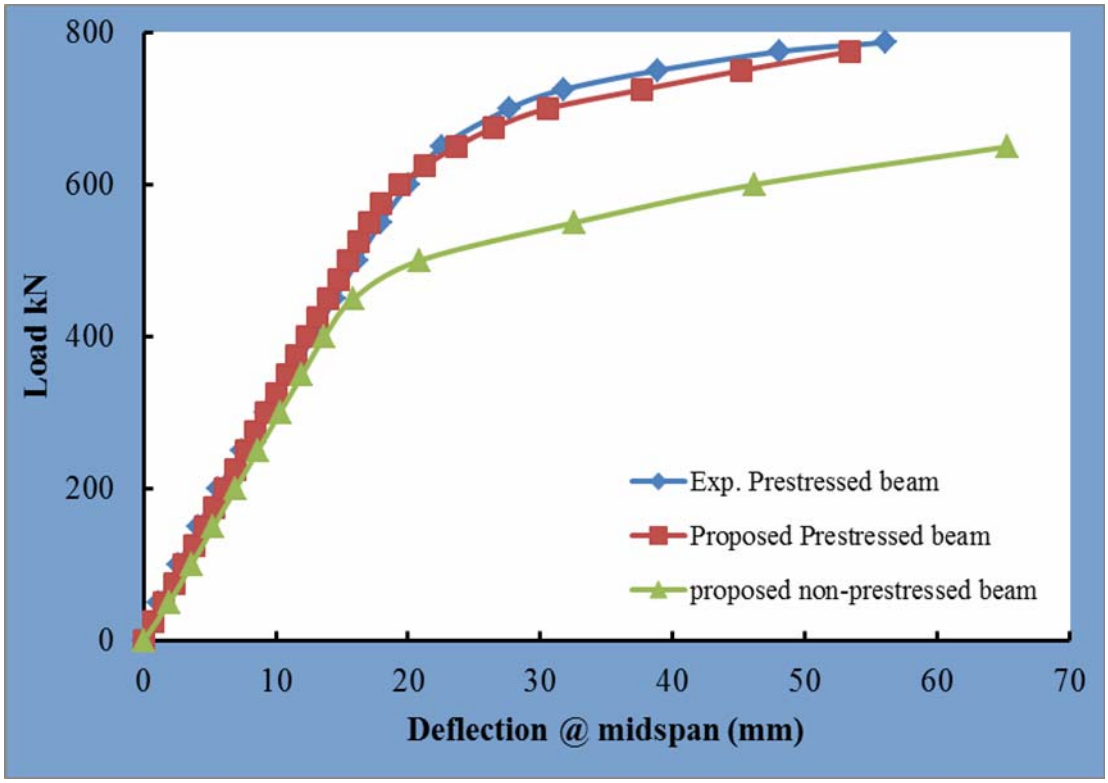

Figure (15): Difference between External and non Prestressed Composite Beams.

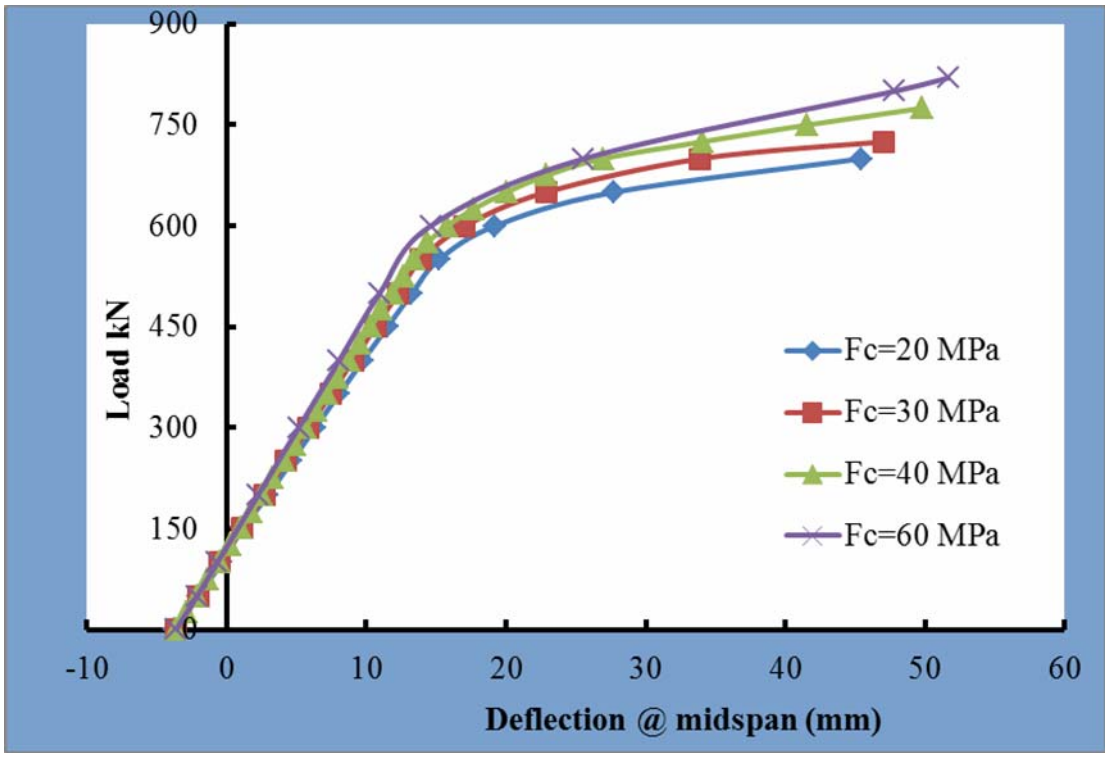

Figure (16): Effect of Compressive Strength of Concrete on the Load-Deflection Behavior of Beam

Table (1): Properties of Beam A, (Ayyub 1990)

Steel Girder Properties	Value
Modulus of Elasticity, E_g(MPa)	200000
Ultimate Stress, f_u (MPa)	565
Yield Stress, f_y (MPa)	411
Ultimate Strain, ε_u	0.22
Area, (mm^2)	5709.66
Reinforcement Steel Properties	**Value**
Modulus of Elasticity, E_g(MPa)	200000
Ultimate Stress, f_u (MPa)	420
Yield Stress, f_y (MPa)	380
Ultimate Strain, ε_u	0.24
Area, (mm^2)	78.54
Modulus of Elasticity E_c (MPa)	29725
Ultimate compressive stress , $\acute{f}_c$ (MPa)	40
Modulus of rupture, f_r (MPa)	4
Strain corresponding to, $\acute{f}_c$, ε_o	0.002
The ratio of elastic strains to the total strains,v	0.5
Prestressing Steel Properties	Value
Modulus of Elasticity, E_g(MPa)	200000
Ultimate Stress, f_u (MPa)	1860
Yield Stress, f_y (MPa)	1680
Ultimate Strain, ε_u	0.09
Area, (mm^2)	180
No. of strands	2
Initial Prestresseing force, (kN) ($2N$) for two strands	289
Initial tendons stress, (MPa)	1035